



Published in final edited form as:

Circ Res. 2008 April 11; 102(7): 752–760. doi:10.1161/CIRCRESAHA.107.159517.

## Periostin Is Required for Maturation and Extracellular Matrix Stabilization of Noncardiomyocyte Lineages of the Heart

Paige Snider, Robert B. Hinton, Ricardo A. Moreno-Rodriguez, Jian Wang, Rhonda Rogers, Andrew Lindsley, Fang Li, David A. Ingram, Donald Menick, Loren Field, Anthony B. Firulli, Jeffery D. Molkentin, Roger Markwald, and Simon J. Conway

From the Cardiovascular Development Group (P.S., J.W., R.R., A.L., F.L., D.A.I., L.F., A.B.F., S.J.C.), Herman B Wells Center for Pediatric Research, Indiana University School of Medicine, Indianapolis; Cincinnati Children's Hospital (R.B.H., J.D.M.), Ohio; and Medical University of South Carolina (R.A.M.-R., D.M., R.M.), Charleston.

### Abstract

The secreted periostin protein, which marks mesenchymal cells in endocardial cushions following epithelial–mesenchymal transformation and in mature valves following remodeling, is a putative valvulogenesis target molecule. Indeed, periostin is expressed throughout cardiovascular morphogenesis and in all 4 adult mice valves (annulus and leaflets). Additionally, periostin is expressed throughout the fibrous cardiac skeleton and endocardial cushions in the developing heart but is absent from both normal and/or pathological mouse cardiomyocytes. Periostin (*peri<sup>lacZ</sup>*) knockout mice exhibit viable valve disease, with neonatal lethality in a minority and latent disease with leaflet abnormalities in the viable majority. Surviving *peri<sup>lacZ</sup>*-null leaflets are truncated, contain ectopic cardiomyocytes and smooth muscle, misexpress the cartilage proteoglycan aggrecan, demonstrate disorganized matrix stratification, and exhibit reduced transforming growth factor- $\beta$  signaling. Neonatal *peri<sup>lacZ</sup>* nulls that die (14%) display additional defects, including leaflet discontinuities, delamination defects, and deposition of acellular extracellular matrix. Assessment of collagen production, 3D lattice formation ability, and transforming growth factor- $\beta$  responsiveness indicate periostin-deficient fibroblasts are unable to support normal valvular remodeling and establishment of a mature cardiac skeleton. Furthermore, pediatric stenotic bicuspid aortic valves that have lost normal extracellular matrix trilaminar stratification have greatly reduced periostin. This suggests that loss of periostin results in inappropriate differentiation of mesenchymal cushion cells and valvular abnormalities via a transforming growth factor- $\beta$ -dependent pathway during establishment of the mature heart. Thus, *peri<sup>lacZ</sup>* knockouts provide a new model of viable latent valve disease.

### Keywords

heart development; periostin; cardiac skeleton; valve; mouse

---

Defects within valves and associated fibrous structures of the heart are the most common congenital defect subtype, accounting for 25% to 30% of all malformations.<sup>1</sup> Despite epidemiology studies showing an increased incidence of valve disease,<sup>2</sup> little is known about

---

© American Heart Association, All rights reserved.

Correspondence to Simon J. Conway, Indiana University, 1044 W Walnut St, Indianapolis, IN 46202. E-mail siconway@iupui.edu . Reprints: Information about reprints can be found online at <http://www.lww.com/reprints>

### Disclosures

None.

its pathogenesis. Recent evidence implicates genetic causes and dysregulation of genes important during valvular development.<sup>3–7</sup> Although some congenital valvular defects are detected at birth, the majority only become apparent later in life and increase the risk of subsequent morbidity and mortality.<sup>1,4</sup>

During heart development, cushion mesenchyme is repositioned and remodeled to form projections that give rise to stress-resistant valves, whereas atrioventricular (AV) mesenchyme gives rise to the annulus that provides anchorage for the mitral and tricuspid leaflets to the working myocardium. Similarly, nonvalvular outflow tract (OFT) mesenchymatous cells populate the fibrous aortic and pulmonary attachment rings. The structural organization of the collagenous extracellular matrix (ECM) network is essential for cardiac function,<sup>8</sup> and the cardiac fibroblast is the principal cell type responsible for producing components of the ECM.<sup>8</sup> Although much is known concerning the organization and function of the fibrous tissue network of the heart,<sup>8</sup> comparatively little is known about the adhesion molecules that maintain valvular ECM homeostasis.

Periostin exhibits structural similarity to fasciclin-I, a *Drosophila* protein involved in neuronal cell–cell adhesion.<sup>9</sup> There are secreted and membrane-associated isoforms of periostin that can act as ligands for select integrins, affecting cell migration, adhesion, and epithelial–mesenchymal transition (EMT) in various normal<sup>10,11</sup> and diseased states.<sup>12</sup> Periostin can also directly interact with other ECM proteins such as collagen type I, collagen type V, fibronectin, tenascin-C, and heparin,<sup>10,13</sup> suggesting periostin plays a critical role in ECM homeostasis. Here, we identified periostin as a valvulogenesis adhesion molecule marking mesenchymal cells in both OFT and AV cushions and within mature leaflets following remodeling.<sup>11,14</sup>

Recently, periostin has been shown to regulate mouse interstitial fibrosis, fibroblast adherence to cardiomyocytes, and ventricular remodeling following pressure overload and myocardial infarction.<sup>10</sup> Additionally, periostin is upregulated in rat carotid arteries following injury and stimulation with transforming growth factor (TGF) $\beta$ <sup>15</sup> and in fibrillin-1 mutant mice exhibiting excessive TGF $\beta$  signaling.<sup>16</sup> Both systemic *TGF $\beta$ 2* (Tom Doetschman, personnel communication) and cardiomyocyte-restricted *Alk3* knockouts exhibit reduced periostin.<sup>17</sup> Collectively, this suggests that periostin may play multiple roles as a primary responder molecule and be linked to ECM deposition and/or reorganization during homeostasis of adult cardiovascular tissues.

To investigate the role of periostin in hearts, we analyzed targeted null mice<sup>18</sup> (*peri<sup>lacZ</sup>*). Our hypothesis was 2-fold: (1) that periostin mediates cushion mesenchyme differentiation into fibroblastic tissue, while inhibiting differentiation into other mesodermal phenotypes; and/or (2) that periostin can act as a collagen-binding protein to modify fibrillogenesis. Here, we show that periostin is dynamically expressed throughout morphogenesis of the fibrous skeleton of the heart and is absent from cardiomyocytes and that expression is upregulated in response to enhanced TGF $\beta$  activity. Both surviving adult and lethal postnatal *peri<sup>lacZ</sup>*-null valves exhibit a spectrum of ECM structural and molecular abnormalities, notably a blunted fibroblast competence to respond to exogenous TGF $\beta$ , suppressed TGF $\beta$  signaling, and inappropriate differentiation of mesenchymal cushions, resulting in ectopic ECM deposits. Furthermore, periostin is greatly reduced in diseased human valves when the ECM is disorganized. Because a complete loss of heart valve/fibrous skeleton structures is rare in newborn human hearts, these studies highlight the importance of matrix homeostasis in the pathogenesis of valvular/annulus defects.

## Materials and Methods

### Mice

*peri<sup>lacZ</sup>* mice<sup>18</sup> were intercrossed with  *$\alpha$ MHC-EGFP* reporter mice that express enhanced green fluorescent protein (EGFP) under control of the cardiac-restricted  $\alpha$  myosin heavy chain ( *$\alpha$ MHC*) promoter.<sup>19</sup> *Foxc1* mutant embryos were harvested from heterozygous intercrosses,<sup>20</sup> and *Smad6* mutants<sup>21</sup> were provided by M. Kern (Medical University of South Carolina).

### Gene Expression Assays, Explant Culture, and Histological Analysis

Histochemistry for  $\beta$ -galactosidase, in situ hybridization, RT-PCR, immunohistochemistry, and histology were performed according to standard protocols.<sup>18</sup> For the cDNA probes, antibodies, and histological stains used, see the online data supplement, available at <http://circes.ahajournals.org>. Mouse embryonic fibroblast (MEF) isolation, 3D collagen cultures, and TGF $\beta$  responsiveness studies were carried out as described previously<sup>22–24</sup> but with minor modifications. See the online supplement for details on procedures.

### Statistical Analysis

Data are presented as means $\pm$ SD of the mean. Student's *t* test was applied for data comparison, and  $P < 0.05$  or  $P < 0.01$  were assigned as significant.

## Results

### Periostin Exhibits Restricted Expression in Developing Cardiac Skeleton and Mature Valve Apparatus

In situ analysis revealed that in addition to expression in endocardial cushions and valve leaflets,<sup>11</sup> periostin is coordinately expressed in the developing and mature cardiac fibrous skeleton. Specifically, periostin mRNA and protein are expressed in cardiac fibroblasts, valvular attachment apparatus, chordae tendineae, and epicardial/pericardial structures but are absent from the cardiomyocyte lineage (Figure 1). Significantly, coincident with initial embryonic day (E)10.5 appearance of mouse cardiac fibroblasts,<sup>8</sup> all 3 embryonically expressed fasciclin-containing genes are expressed (Figure I in the online data supplement). Western blot analysis using a polyclonal  $\alpha$ -periostin antibody that detects all known isoforms,<sup>25</sup> reveals periostin levels increase coincident with increasing fibroblast content (Figure 1).<sup>26</sup> Protein spatiotemporal expression correlates with mRNA expression in the fibrous skeleton but exhibits a restricted pattern within the leaflets (Figure 1). Restriction occurs before cushion remodeling and fibrous differentiation (supplemental Figure II), suggesting the involvement of periostin in providing a permissive, spatially defined ECM promoting proper organization of nascent cushion ECM. Robust periostin expression is present in mature load-bearing collagenous central fibrosa, suggestive of a structural integrity role during maintenance of unidirectional flow.

### Periostin Is Absent From Cardiomyocytes but Is Expressed Throughout the Rest of the Heart

Because elevated periostin expression is present following adult myocardial hypertrophy,<sup>10</sup> infarction,<sup>27</sup> arterial injury,<sup>15</sup> and valve calcification,<sup>28</sup> we examined its expression in both normal and heart failure models to assess when and where periostin elevation occurs. To efficiently distinguish cardiomyocytes from the noncardiomyocyte cells, we made use of the  *$\alpha$ MHC-EGFP* reporter mice<sup>19</sup> expressing EGFP exclusively in cardiac muscle. In wild-type ventricles and atria, periostin is absent from EGFP-expressing cardiomyocytes but expressed within noncardiomyocytes (primarily fibroblasts) and vascular smooth muscle cells (Figure 2). Periostin colocalizes in vivo and in vitro with collagen type I and discoidin-domain receptor<sup>28</sup> (data not shown) but, again, is not detected in MF20-positive and sarcomeric actin-

positive cardiomyocytes (Figure 2A through 2F). Significantly, periostin ImmunoGold immunohistochemistry and biochemical coimmunoprecipitation demonstrated periostin decorates collagen fibrils by directly binding collagen type I.<sup>13</sup> Similarly, in isolated fetal cardiac fibroblasts, periostin is coexpressed with collagen type I within the cytoplasmic endoplasmic reticulum/Golgi, indicative of active synthesis (Figure 2G and 2H). Because periostin is expressed as both secreted and matrix-bound isoforms,<sup>25</sup> it was unclear from previous reports whether fibroblasts actually secrete periostin. Immunoblotting of fetal cardiac fibroblasts and culture media reveals periostin is secreted by periostin-expressing fibroblasts (Figure 2I). As analysis of *peri<sup>lacZ</sup>*-null fibroblast supernatant was negative, indicating we that we were detecting periostin directly secreted via cells (data not shown). Furthermore, because periostin is known to be TGF $\beta$  responsive,<sup>16</sup> TGF $\beta$  neutralization antibodies can inhibit stretch-induced periostin upregulation,<sup>27</sup> and periostin mRNA expression can be stimulated by TGF $\beta$ 1 in cultured vascular smooth muscle cells,<sup>15</sup> we assessed periostin expression and TGF $\beta$ 1 responsiveness in cultured fetal (E14) and newborn isolated cardiac fibroblasts and cardiomyocytes. Indeed, periostin is expressed and upregulated within only cardiac fibroblasts in response to exogenous TGF $\beta$ 1 but not in cardiomyocytes (Figure 2J). To assess whether periostin expression remains restricted to the noncardiomyocyte lineages during pathological insult, we analyzed expression in 2 heart failure models. Consistent with hypertrophy data,<sup>10</sup> elevated periostin protein was only observed in activated fibroblasts and not within adjacent cardiomyocytes (supplemental Figure III). Taken together, these data support previous reports<sup>10,11,13,14,17,18,29</sup> that periostin is undetectable in mouse, rat, or chick cardiomyocytes.

### Viable *peri<sup>lacZ</sup>* Valve Annuli and Leaflets Are Hypoplastic

As expected, histological analysis of E13.5 and E16 null hearts did not reveal structural abnormalities, because *peri<sup>lacZ</sup>* nulls are present at expected Mendelian ratios at birth.<sup>18</sup> Analysis of surviving adult *peri<sup>lacZ</sup>* nulls revealing that they often exhibit a bulging right ventricle, particularly within the OFT region, may be indicative of abnormal semilunar valves (Figure 3b). Histology reveals that 100% of null (n=8/8 sectioned) mitral and tricuspid leaflets are significantly shorter and thickened compared with wild-type littermates (Figure 3b; see the online data supplement for further details). Subsequent analysis of proliferation index and cell density in wild-type and *peri<sup>lacZ</sup>*-null littermates containing the  *$\alpha$ MHC-EGFP* cardiomyocytes reporter indicated that null cushions are initially formed normally, and exhibit equivalent proliferation and have similar cell densities, compared with wild types (see the online data supplement for further details). Furthermore, histomorphometric analysis of 4-month-old *peri<sup>lacZ</sup>*-null and littermate control hearts (n=6 of each genotype) revealed that fibroblast cell numbers and total cellularity were unaffected by loss of periostin (see the online data supplement for further details).

Significantly, surviving *peri<sup>lacZ</sup>*-null short leaflets also contained ectopic  *$\alpha$ MHC-EGFP* because EGFP-positive islands are present in null mitral and tricuspid leaflets (supplemental Figure IV). Isolated null leaflets can spontaneously undergo twitching, further suggesting that myocardial tissue is present. This was confirmed via expression of myocardial-specific MF20 in *peri<sup>lacZ</sup>*-null but not wild-type leaflets (Figure 4A through 4D). Additionally, we found ectopic clusters of  $\alpha$  smooth muscle actin (SMA)-positive cells in some null leaflets, confirming the presence of abnormal intermediate cell lineages (supplemental Figure IV). Thus, abnormally muscularized null mitral and tricuspid valves may secondarily result in valvular dysfunction.

To understand the molecular pathway giving rise to null anomalies, we used RT-PCR to identify differentially expressed target genes. Interestingly, adult *peri<sup>lacZ</sup>* nulls fail to downregulate aggrecan (Figure 4E through 4G) but exhibit normal expression of alkaline phosphatase (osteoblast marker), fibulin-1c/d (aggrecan ligands), and versican (cartilage

proteoglycan) expression. Aggrecan is a large chondroitin-sulfate proteoglycan, a major structural component in cartilage matrix also exhibiting dynamic expression in valves.<sup>30</sup> Specifically, aggrecan mRNA and protein are localized in the embryo mesenchymal endocardial OFT and AV cushions but downregulated in neonates and absent from normal adult mice hearts.<sup>30</sup> Recently, it was proposed that *Sox9/Bmp2* regulation of aggrecan may be required for valve remodeling.<sup>4</sup> In tendons (closest to valves in terms of tissue-type), the relative proportion of collagen:proteoglycan determines tissue type<sup>31</sup>; thus continued aggrecan expression could result in altered null valve viscoelastic properties or represent lack of appropriate cushion differentiation. Also significant, the related *βigH3* gene<sup>14</sup> is normally expressed in adult nulls, suggesting it is unlikely *βigH3* upregulation compensates for postnatal loss of periostin. However, it is unknown whether *βigH3* can functionally compensate for loss of periostin in utero.

To identify where and when *peri<sup>lacZ</sup>*-null hearts are affected, we assessed in utero morphogenesis and neonatal remodeling. Histology of embryonic (E10 to E12) and fetal (E14 to E18) hearts did not reveal structural anomalies, and *Nfatc1* is appropriately expressed in null fetal endocardium overlying the developing endocardial cushions (data not shown). Expression of *Nfatc1* is usually extinguished once EMT has occurred,<sup>5</sup> indicating that, unlike *Foxp1* mutants exhibiting ectopic *Nfatc1*,<sup>32</sup> the *peri<sup>lacZ</sup>*-null cushions form normally. However, we observed increases in glycosaminoglycans in *peri<sup>lacZ</sup>*-null E12 cushions (Figure 5B) until E16. Histological analysis of neonatal (1 to 3 weeks) and adult valves revealed loss of trilaminar organization and hypoplastic annuli but unaltered platelet endothelial cell adhesion molecule expression, indicating presence of intact endothelium (Figure 5). Collectively, these results demonstrate that cushion formation is not altered but inappropriate *peri<sup>lacZ</sup>*-null cushion differentiation and that abnormal late valve remodeling results in viable valvular defects.

### Valvular Insufficiency Underlies Neonatal Lethality

In contrast, analysis of nulls dying before weaning ( $\approx 14\%$ ) revealed gross cardiac architectural and valvular anomalies (Figure 3c). Their neonatal hearts are abnormally shaped, and mitral/tricuspid leaflets are shorter than those in surviving nulls. Histology revealed that some null mitral valves are partially tethered to the septum. We also observed sporadic large acellular amorphous ECM deposits in thickened mitral/tricuspid leaflets, resulting in discontinuities in the valves. Alcian blue staining (detects valvular mucopolysaccharides) indicates that deposits are mucopolysaccharides, further supporting the hypothesis that in the absence of periostin, cushion differentiation is abnormal. Given the size and position of deposits, the appearance of ectopic  $\alpha$ SMA/MF20-positive cells, and increased aggrecan, it is likely that decreased structural integrity is the most probable cause of lethality in this subpopulation of *peri<sup>lacZ</sup>*-null neonates. *peri<sup>lacZ</sup>*-null lethality is only partially penetrant, suggesting modifier effects (ie, background, redundancy, and/or genetic interactions) are responsible for neonatal death.

### Periostin Is TGF $\beta$ -Responsive

Given that differentiation along inappropriate pathways occurs in the absence of periostin and that it is linked to TGF $\beta$ -superfamily signaling, we analyzed *Smad6* knockouts. Targeted deletion of the *Smad6*-negative regulator of TGF $\beta$  signaling revealed that it is required for valve maturation and suppression of osteogenesis within endocardial cushions.<sup>21</sup> In situ revealed that periostin is upregulated in *Smad6* nulls exhibiting valvular hyperplasia (Figure 6A). Thus, altered TGF $\beta$ /*Smad6* signaling is upstream and may modulate periostin, because when inhibitory Smads are removed (leading to elevated TGF $\beta$  signaling), periostin is also upregulated. In support of this, periostin expression is downregulated in *Foxc1* nulls failing to undergo TGF $\beta$ -mediated mesenchymal maturation (Figure 6A). *Foxc1* is a TGF $\beta$ 1-responsive gene, and null embryos exhibit valve hypoplasia resulting from mesenchymal maturation



defects.<sup>20</sup> Furthermore, we recently identified a 3.9-kb periostin enhancer containing both TGF $\beta$ -responsive and bone morphogenetic protein (BMP)-responsive elements expressed in OFT cushions.<sup>33</sup> However, a 304-bp periostin minimal element, still capable of in vivo cushion expression, requires only TGF $\beta$ - but not BMP-responsive elements.<sup>33</sup> Similarly, we demonstrated *Bmp4*-null cushions express periostin,<sup>25</sup> suggesting that *Bmp4* (and possibly other *Bmp* genes) is not required for periostin OFT expression.

To directly test in vivo TGF $\beta$  responsiveness in mature hearts, we assessed expression in cardiac-restricted  *$\alpha$ MHC-TGF $\beta$ 1* constitutively active mice.<sup>34</sup> Increased TGF $\beta$ 1-activity was observed during pathological cardiac remodeling in various animal models, but surprisingly, overt fibrosis was only observed in the atria when a TGF $\beta$ 1 latent complex was tethered to the ECM.<sup>34</sup> These data indicate increased TGF $\beta$ 1 activity alone is insufficient to promote ventricular fibrosis in adult ventricle.<sup>34</sup> Supporting our hypothesis, periostin protein is upregulated in adult TGF $\beta$ 1 transgenic-positive hearts (Figure 6B), indicating TGF $\beta$ 1 activation directly correlates with periostin upregulation and can occur without fibrosis. To further assess whether there is altered TGF $\beta$ -signaling activity in *peri<sup>lacZ</sup>*-null leaflets, we performed immunohistochemistry with anti-phosphorylated Smad2,3 antibody, a marker of TGF $\beta$  signaling.<sup>35</sup> At E14.0, mutant endocardial cushions/ leaflets exhibited markedly reduced pSmad2,3 expression before definitive leaflet remodeling (Figure 6E and 6F).

Because we have shown that periostin can directly bind collagen type I,<sup>13</sup> we measured collagen synthesis in wild-type and *peri<sup>lacZ</sup>*-null MEFs alone or coincubated with exogenously supplied TGF $\beta$ . When equivalent MEFs were compared, *peri<sup>lacZ</sup>* nulls synthesized  $\approx$ 32% less collagen than wild types and failed to respond proportionately to added TGF $\beta$  (Figure 6C). This indicates that periostin possibly signals fibroblasts to secrete collagen or that it can bind to collagen, thereby decreasing its removal from the ECM. Given the reduced TGF $\beta$ -signaling activity and observed ECM disorganization abnormalities in *peri<sup>lacZ</sup>* nulls, we evaluated the ability of null MEFs to reorganize and contract 3D collagen lattices and their response to exogenous TGF $\beta$ . Collagen gel contraction assays<sup>23,24</sup> were used to quantitatively examine the effect of periostin on alignment and condensation of preexisting fibrils analogous to what may be occurring in vivo when cushions become attenuated into cusps by the compactations and organization of fibrils and other ECM components into stratified layers of dense regular fibrous tissue. Significantly, *peri<sup>lacZ</sup>*-null MEFs exhibit reduced reorganization, contraction ability (Figure 6D), and statistically diminished response to increasing TGF $\beta$  (supplemental Figure VI). This further indicates a defect in the *peri<sup>lacZ</sup>*-null valvular and nonvalvular fibroblasts that blunts TGF $\beta$  responsiveness, resulting in an altered ECM.

### Periostin Is Greatly Reduced in Diseased Human Valves

Given the localization of periostin within the collagen-rich fibrosa layer of the valve (Figure 1F), expression studies were extended to human tissue to evaluate periostin in valve disease (Figure 7). In explanted pediatric valve tissue<sup>4</sup> from thickened stenotic aortic valves, periostin expression was significantly reduced compared with age-matched controls, correlating with loss of ECM trilaminar stratification, disorganized collagen, and cellular disarray observed in these diseased valves.<sup>4</sup> Periostin expression in normal valve tissue is robust in the fibrosa and glycosaminoglycan-containing spongiosa layers and weakly positive in the ventricularis layer. Taken together, these findings complement the mouse in vivo and in vitro analyses and suggest that periostin has a role in human valve disease pathogenesis, warranting further investigation.

### Discussion

Although the cellular and molecular mechanisms underlying cushion remodeling and formation of the fibrous skeleton of the heart are complex and depend on multiple gene networks, these data demonstrate periostin is an intriguing matrix effector protein that is

required for normal ECM deposition within the heart. Furthermore, not only is periostin directly induced via TGF $\beta$  but is required for normal TGF $\beta$  signaling and TGF $\beta$  responsiveness during in utero cardiac fibroblast, valvular ECM organization, and postnatal homeostasis (Figure 8). During myocardial injury, periostin is significantly upregulated coincident with TGF $\beta$ -mediated ECM deposition.<sup>10,29</sup> Significantly, we demonstrated TGF $\beta$ 1-induced periostin upregulation can occur in the absence of ventricular fibrosis. Thus, our data suggest direct correlation between TGF $\beta$ 1 pathway transduction and periostin upregulation, also observed in individuals with Marfan syndrome and fibrillin 1-deficient mice.<sup>16</sup> Select manifestations of Marfan syndrome reflect excessive TGF $\beta$  signaling, resulting in increased Smad2 phosphorylation and consequent periostin upregulation. Inversely, when TGF $\beta$  activity is abrogated using TGF $\beta$ -neutralizing antibodies,<sup>27</sup> targeted knockouts, and the angiotensin II type1 receptor blocker Losartan,<sup>16</sup> expression of normal and pathological periostin is greatly reduced. This suggests periostin may be required to enhance the fibrotic remodeling effects of TGF $\beta$  and stabilize microfibril networks within the cardiac skeleton. Our 3D lattice formation ability assays suggest that secreted periostin acts as a scaffold binding protein to remodel collagen in response to TGF $\beta$ , promoting further periostin expression, collagen synthesis, and periostin binding to collagen, increasing cross-linking and fibrillogenesis.<sup>13</sup> We do not believe that periostin produces or stimulates ECM secretion; rather, its absence may result in an ECM that does not support a reorganized laminar structure.

These data do not formally rule out Bmp pathway involvement in regulation of periostin. Because Bmp genes are predominantly expressed in adjacent myocardium and most TGF $\beta$ -members are predominantly coexpressed with periostin in cushions themselves, this suggests more likely a direct interaction, compared with the possible indirect effects observed in *Alk3* conditional mutants.<sup>17</sup> Recent data indicate that periostin may induce reentry of differentiated mammalian cardiomyocytes into the cell cycle.<sup>36</sup> However, our mouse<sup>10,11,14,17</sup> and chick<sup>13</sup> data and nonphysiological truncated form of periostin used<sup>36</sup> do not support this. Indeed, expression of full-length periostin in adult rat heart using a plasmid-transfection approach induced disease indices, suggesting the bacterially generated truncated periostin used<sup>36</sup> may have had aberrant effects.<sup>29</sup>

Our analysis revealed that 100% of adult *peri<sup>lacZ</sup>*-null leaflets are undersized, lack trilaminar ECM organization, misexpress the chondrogenic marker aggrecan, and undergo abnormal differentiation. Notably, lack of periostin resulted in the presence of ectopic smooth muscle and cardiogenic lineages within valves. This is consistent with the islands/ pockets of fibrosis reported in adult valves including mice and human<sup>37</sup> and *Smad6* knockout phenotypes in which cartilage, bone, marrow, and even blood cells were formed within both AV and aortic valves.<sup>21</sup> Although it is tempting to speculate that periostin may be required to promote and/or maintain differentiation of condensed mesenchyme into connective tissue and inhibit the chondrogenic and myocardial pathways, it is currently unclear whether genetic redundancy among the fasciclin family obscures the in utero function of periostin or whether loss of periostin expression at the myocardial-endocardial cushion interface results in irregular delamination, inadvertently trapping nonvalvular cell types. Although the functional consequence of these ectopic cell types has yet to be determined, aspects of these anomalies are similar to those in mice treated with serotonin agonists that increase TGF $\beta$ 1 activity and collagen biosynthesis, resulting in presence of ectopic  $\alpha$ SMA cells expressing latent TGF $\beta$ -associated peptide.<sup>38</sup> Thus, valves can have subtle malformations that may cause latent clinically significant valve disease (eg, fibrillin 1 in Marfan syndrome,<sup>16,39</sup> TGFBR1/TGFBR2 in Marfan-like disorders,<sup>39</sup> mitral valve prolapse) because small changes over time can cause significant pathology.

Similar to the changes in connective tissue integrity observed in *peri<sup>lacZ</sup>*-null leaflets, periostin expression is also lost in diseased pediatric cardiac valves exhibiting a disorganized ECM.

Whether periostin loss is a primary or secondary finding of dysplastic valvular interstitial cells or whether it directly results in failure of maintenance of valve function, leading to subsequent hyperproliferation and ECM dysregulation, is presently unknown. The ability of the fibrous cardiac skeleton to absorb and distribute the mechanical load during function greatly determines cardiac homeostasis. The fact periostin can directly bind collagen type I<sup>13</sup> (among the most abundant ECM proteins in the cardiac skeleton that provides tensile strength), suggests that it may play a regulatory role in maintaining structural integrity of the heart and valves. This is consistent with data demonstrating that periostin is required for maintenance of periodontal ligament ECM integrity and absorption of mechanical occlusal stresses.<sup>18</sup> Because valvular defects are chronic rather than acute and often not diagnosed until after birth, the *peri<sup>lacZ</sup>* nulls represent a useful model of abnormal valve development leading to latent valve disease.

## Supplementary Material

Refer to Web version on PubMed Central for supplementary material.

## Acknowledgments

### Sources of Funding

This work was supported, in part, by the NIH (to S.J.C., A.B.F., and J.D.M.), T32 HL079995 Training Grant in Vascular Biology and Medicine (to P.S.), and the Indiana University Department of Pediatrics/Cardiology (to S.J.C.).

## References

1. Loffredo CA. Epidemiology of cardiovascular malformations: prevalence and risk factors. *Am J Med Genet* 2000;97:319–325. [PubMed: 11376444]
2. Supino PG, Borer JS, Yin A, Dillingham E, McClymont W. Epidemiology of valvular heart diseases: the problem is growing. *Adv Cardiol* 2004;41:9–15. [PubMed: 15285213]
3. Garg V, Muth AN, Ransom JF, Schluterman M, Barnes R, King IN, Grossfeld PD, Srivastava D. Mutations in NOTCH1 cause aortic valve disease. *Nature* 2005;437:270–274. [PubMed: 16025100]
4. Hinton RB Jr, Lincoln J, Deutsch GH, Osinska H, Manning PB, Benson DW, Yutzey KE. Extracellular matrix remodeling and organization in developing and diseased aortic valves. *Circ Res* 2006;98:1431–1438. [PubMed: 16645142]
5. Zhou B, Wu B, Tompkins KL, Boyer KL, Grindley JC, Baldwin HS. Characterization of Nfatc1 regulation identifies an enhancer required for gene expression that is specific to pro-valve endocardial cells in developing heart. *Development* 2005;132:1137–1146. [PubMed: 15689382]
6. Armstrong EJ, Bischoff J. Heart valve development: endothelial cell signaling and differentiation. *Circ Res* 2004;95:459–470. [PubMed: 15345668]
7. Chang CP, Neilson JR, Bayle JH, Gestwicki JE, Kuo A, Stankunas K, Graef IA, Crabtree GR. Field of myocardial-endocardial NFAT signaling underlies heart valve morphogenesis. *Cell* 2004;118:649–663. [PubMed: 15339668]
8. Goldsmith EC, Hoffman A, Morales MO, Potts JD, Price RL, McFadden A, Rice M, Borg TK. Organization of fibroblasts in heart. *Dev Dyn* 2004;230:787–794. [PubMed: 15254913]
9. Takeshita S, Kikuno R, Tezuka K, Amann E. Osteoblast-specific factor-2: cloning of a putative bone adhesion protein with homology with insect protein fasciiclin-I. *Biochem J* 1993;294:271–278. [PubMed: 8363580]
10. Oka T, Xu J, Kaiser RA, Melendez J, Hambleton M, Sargent MA, Lorts A, Brunskill EW, Dorn GW, Conway SJ, Aronow BJ, Robbins J, Molkentin JD. Genetic manipulation of periostin expression reveals a role in cardiac hypertrophy and ventricular remodeling. *Circ Res* 2007;101:313–321. [PubMed: 17569887]



11. Kruzynska-Frejtag A, Machnicki M, Rogers R, Markwald RR, Conway SJ. Periostin is expressed in the embryonic mouse heart during valve formation. *Mech Dev* 2001;103:183–188. [PubMed: 11335131]
12. Bao S, Ouyang G, Bai X, Huang Z, Ma C, Liu M, Shao R, Anderson RM, Rich JN, Wang XF. Periostin potently promotes metastatic growth of colon cancer by augmenting cell survival via Akt/PKB pathway. *Cancer Cell* 2004;5:329–339. [PubMed: 15093540]
13. Norris R, Damon B, Mironov V, Kasyanov V, Ramamurthi R, Moreno-Rodriguez R, Trusk T, Potts J, Goodwin R, Davis J, Hoffman S, Wen X, Sugi Y, Kern K, Mjaatvedt C, Turner D, Oka T, Conway SJ, Molkentin J, Forgacs G, Markwald RR. Periostin regulates collagen fibrillogenesis and biomechanical properties of connective tissues. *J Cell Biochem* 2007;101:695–711. [PubMed: 17226767]
14. Lindsley A, Li W, Wang J, Maeda N, Rogers R, Conway SJ. Comparison of four mouse fasciclin-containing genes expression patterns during valvuloseptal morphogenesis. *Gene Expr Patterns* 2005;5:593–600. [PubMed: 15907457]
15. Li G, Oparil S, Sanders JM, Zhang L, Dai M, Chen LB, Conway SJ, McNamara CA, Sarembock IJ. Phosphatidylinositol-3-kinase signaling mediates VSMC expression of periostin in vivo and in vitro. *Atherosclerosis* 2006;188:292–300. [PubMed: 16325820]
16. Cohn RD, van Erp C, Habashi JP, Soleimani AA, Klein EC, Lisi MT, Gamradt M, Rhys CM, Holm TM, Loeys BL, Ramirez F, Judge DP, Ward CW, Dietz HC. Angiotensin II type 1 receptor blockade attenuates TGF-beta-induced failure of muscle regeneration in multiple myopathic states. *Nat Med* 2007;13:204–210. [PubMed: 17237794]
17. Gaussin V, Morley GE, Cox L, Zwijssen A, Vance KM, Emile L, Tian Y, Liu J, Hong C, Myers D, Conway SJ, Depre C, Mishina Y, Behringer RR, Hanks MC, Schneider MD, Huylebroeck D, Fishman GI, Burch JB, Vatner SF. Alk3/Bmpr1a receptor is required for development of the atrioventricular canal into valves and annulus fibrosus. *Circ Res* 2005;97:219–226. [PubMed: 16037571]
18. Rios H, Koushik SV, Wang H, Wang J, Zhou HM, Lindsley A, Rogers R, Chen Z, Maeda M, Kruzynska-Frejtag A, Feng JQ, Conway SJ. Periostin null mice exhibit dwarfism, incisor enamel defects, and an early-onset periodontal disease-like phenotype. *Mol Cell Biol* 2005;25:11131–11144. [PubMed: 16314533]
19. Rubart M, Pasumarthi KB, Nakajima H, Soonpaa MH, Nakajima HO, Field LJ. Physiological coupling of donor and host cardiomyocytes after cellular transplantation. *Circ Res* 2003;92:1217–1224. [PubMed: 12730096]
20. Winnier G, Kume T, Deng K, Rogers R, Bundy J, Raines C, Hogan B, Conway SJ. Roles for the winged-helix-transcription factors MF1 and MFH1 in cardiovascular development revealed by non-allelic non-complementation of null alleles. *Dev Biol* 1999;216:16–27. [PubMed: 10588860]
21. Galvin KM, Donovan MJ, Lynch CA, Meyer RI, Paul RJ, Lorenz JN, Fairchild-Huntress V, Dixon KL, Dunmore JH, Gimbrone MA Jr, Falb D, Huszar D. A role for Smad6 in development and homeostasis of the cardiovascular system. *Nat Genet* 2000;4:171–174. [PubMed: 10655064]
22. Borg TK, Rubin K, Lundgren E, Borg K, Obrink B. Recognition of extracellular matrix components by neonatal and adult cardiac myocytes. *Dev Biol* 1984;104:86–96. [PubMed: 6734942]
23. Kanekar S, Borg TK, Terracio L, Carver W. Modulation of heart fibroblast migration and collagen gel contraction by IGF-I. *Cell Adhes Commun* 2000;7:513–523. [PubMed: 11051461]
24. Yang FC, Chen S, Clegg T, Li X, Morgan T, Estwick SA, Yuan J, Khalaf W, Burgin S, Travers J, Parada LF, Ingram DA, Clapp DW. Nf1<sup>+/-</sup> mast cells induce neurofibroma-like phenotypes through secreted TGF-beta signaling. *Hum Mol Genet* 2006;15:2421–2437. [PubMed: 16835260]
25. Kruzynska-Frejtag A, Wang J, Maeda M, Rogers R, Krug E, Hoffman S, Markwald R, Conway SJ. Periostin is expressed in the developing teeth at the sites of epithelial-mesenchymal interaction. *Dev Dyn* 2004;229:857–868. [PubMed: 15042709]
26. Soonpaa M, Kim K, Pajak L, Franklin M, Field LJ. Cardiomyocyte DNA synthesis and binucleation during murine development. *Am J Physiol* 1996;271:H2183–H2189. [PubMed: 8945939]
27. Iekushi K, Taniyama Y, Azuma J, Katsuragi N, Dosaka N, Sanada F, Koibuchi N, Nagao K, Ogihara T, Morishita R. Novel mechanisms of valsartan on treatment of acute myocardial infarction through inhibition of anti-adhesion molecule periostin. *Hypertension* 2007;49:1409–1414. [PubMed: 17485602]

28. Osman L, Chester AH, Sarathchandra P, Latif N, Meng W, Taylor PM, Yacoub MH. A novel role of sympatho-adrenergic system in regulating valve calcification. *Circulation* 2007;116:1282–1287. [PubMed: 17846318]
29. Katsuragi N, Morishita R, Nakamura N, Ochiai T, Taniyama Y, Hasegawa Y, Kawashima K, Kaneda Y, Ogihara T, Sugimura K. Periostin as a novel factor responsible for ventricular dilation. *Circulation* 2004;110:1806–1813. [PubMed: 15381649]
30. Zanin MKB, Bundy J, Ernst HJ, Wessels A, Conway SJ, Hoffman S. Distinct spatial and temporal distributions of aggrecan and versican in the embryonic chick heart. *Anat Rec* 1999;256:366–380. [PubMed: 10589023]
31. Vogel KG, Peters JA. Histochemistry defines a proteoglycan-rich layer in bovine flexor tendon subjected to bending. *J Musculoskelet Neuronal Interact* 2005;5:64–69. [PubMed: 15788872]
32. Wang B, Weidenfeld J, Lu MM, Maika S, Kuziel WA, Morrissey EE, Tucker PW. Foxp1 regulates cardiac outflow tract, endocardial-cushion morphogenesis and myocyte proliferation and maturation. *Development* 2004;131:4477–4487. [PubMed: 15342473]
33. Lindsley A, Snider P, Zhou H, Rogers R, Wang J, Olaopa M, Kruzynska-Freitag A, Koushik SV, Lilly B, Burch JB, Firulli AB, Conway SJ. Identification and characterization of a novel Schwann and outflow tract endocardial-cushion lineage-restricted periostin enhancer. *Dev Biol* 2007;307:340–355. [PubMed: 17540359]
34. Nakajima H, Nakajima HO, Salcher O, Dittie AS, Dembowski K, Jing S, Field LJ. Atrial but not ventricular fibrosis in mice expressing a mutant TGF-beta(1) transgene in the heart. *Circ Res* 2000;86:571–579. [PubMed: 10720419]
35. de Sousa Lopes SM, Carvalho RL, van den Driesche S, Goumans MJ, ten Dijke P, Mummery CL. Distribution of phosphorylated Smad2 identifies target tissues of TGF-beta ligands in mouse development. *Gene Expr Patterns* 2003;3:355–360. [PubMed: 12799085]
36. Ku`hn B, del Monte F, Hajjar RJ, Chang YS, Lebeche D, Arab S, Keating MT. Periostin induces proliferation of differentiated cardiomyocytes and promotes cardiac repair. *Nat Med* 2007;13:962–969. [PubMed: 17632525]
37. Mulholland DL, Gotlieb AI. Cell biology of valvular interstitial cells. *Can J Cardiol* 1996;12:231–236. [PubMed: 8624972]
38. Jian B, Xu J, Connolly J, Savani RC, Narula N, Liang B, Levy RJ. Serotonin mechanisms in heart valve disease I: serotonin-induced up-regulation of TGF-beta1 via G-protein signal transduction in aortic valve interstitial cells. *Am J Pathol* 2002;161:2111–2121. [PubMed: 12466127]
39. Dietz HC, Loeys B, Carta L, Ramirez F. Recent progress towards a molecular understanding of Marfan syndrome. *Am J Med Genet C Semin Med Genet* 2005;139:4–9. [PubMed: 16273535]

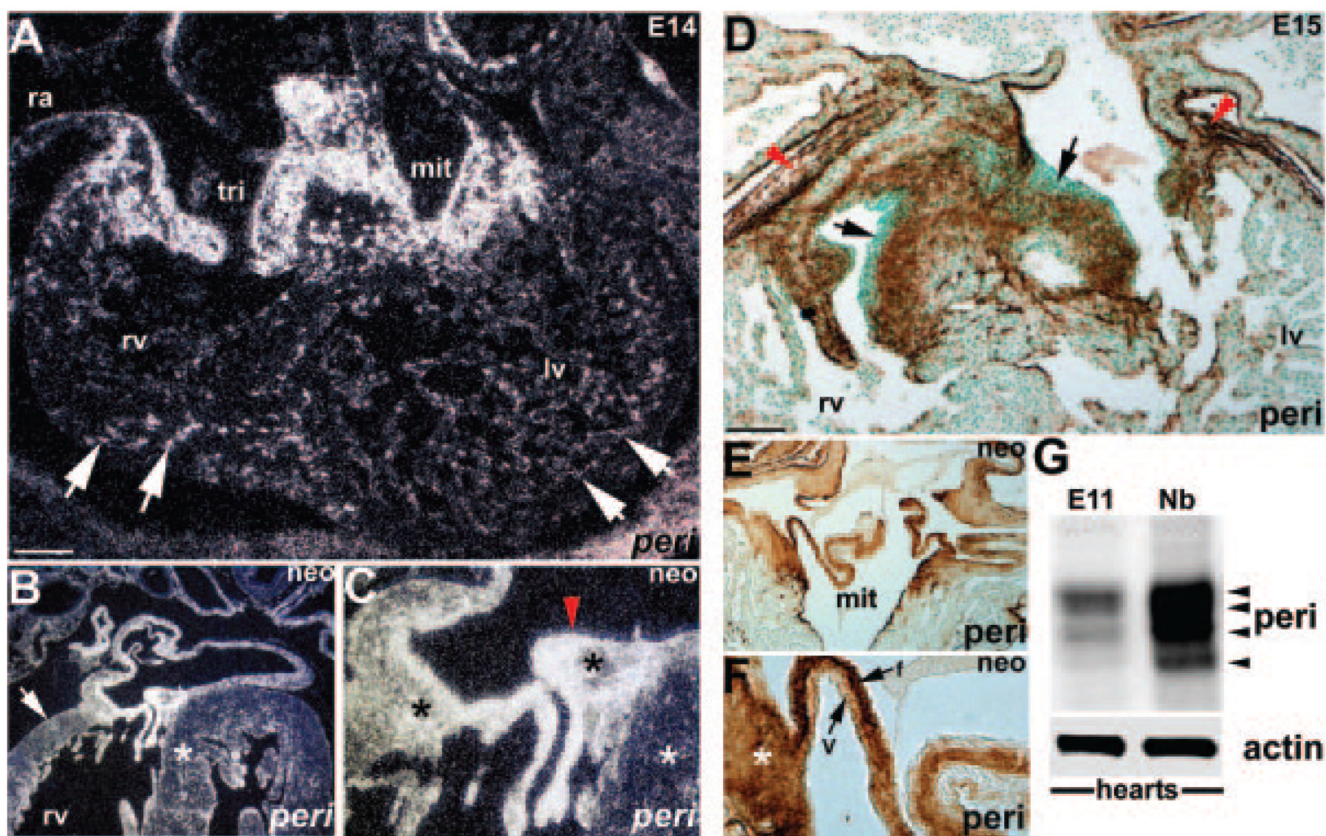


**Figure 1.**

Periostin in developing mouse heart. A through C, In situ reveals periostin (peri) (white grains in darkfield) is expressed throughout the developing cardiac skeleton and endocardial cushions but is absent from endothelium (red arrowhead) (C) and cardiomyocytes. D through F, Immunohistochemistry similarly shows periostin (brown diaminobenzidine substrate) is expressed throughout cardiac skeleton, epicardium (red arrowheads) (D), and most valvular cushion cells but is absent from endothelial cells and cardiomyocytes. In E15 valves (D), periostin is predominately localized to inner cushion regions abutting cardiomyocytes (arrows in D). Robust expression is seen in cardiac fibroblasts and developing annulus (asterisk in F). Neonatal expression is restricted to fibrous (f) rib of mature leaflet and largely absent from ventricularis (V) layer (E and F). G, Western reveals relative levels of periostin increase as the heart undergoes maturation. In E11 hearts (n=4 pooled hearts), only 3 isoforms are weakly present (largest is  $\approx 90$  kDa), but all 4 isoforms ( $\approx 90$ , 87, 85, and 82 kDa) are readily detectable in newborns (Nb) (n=3 pooled hearts). Note actin ( $\approx 42$  kDa) is equally expressed and serves as a loading control. Scale bars, 200  $\mu$ m (A and D). lv, left ventricle; mit, mitral; neo, neonatal; ra, right atria; rv, right ventricle; tri, tricuspid.



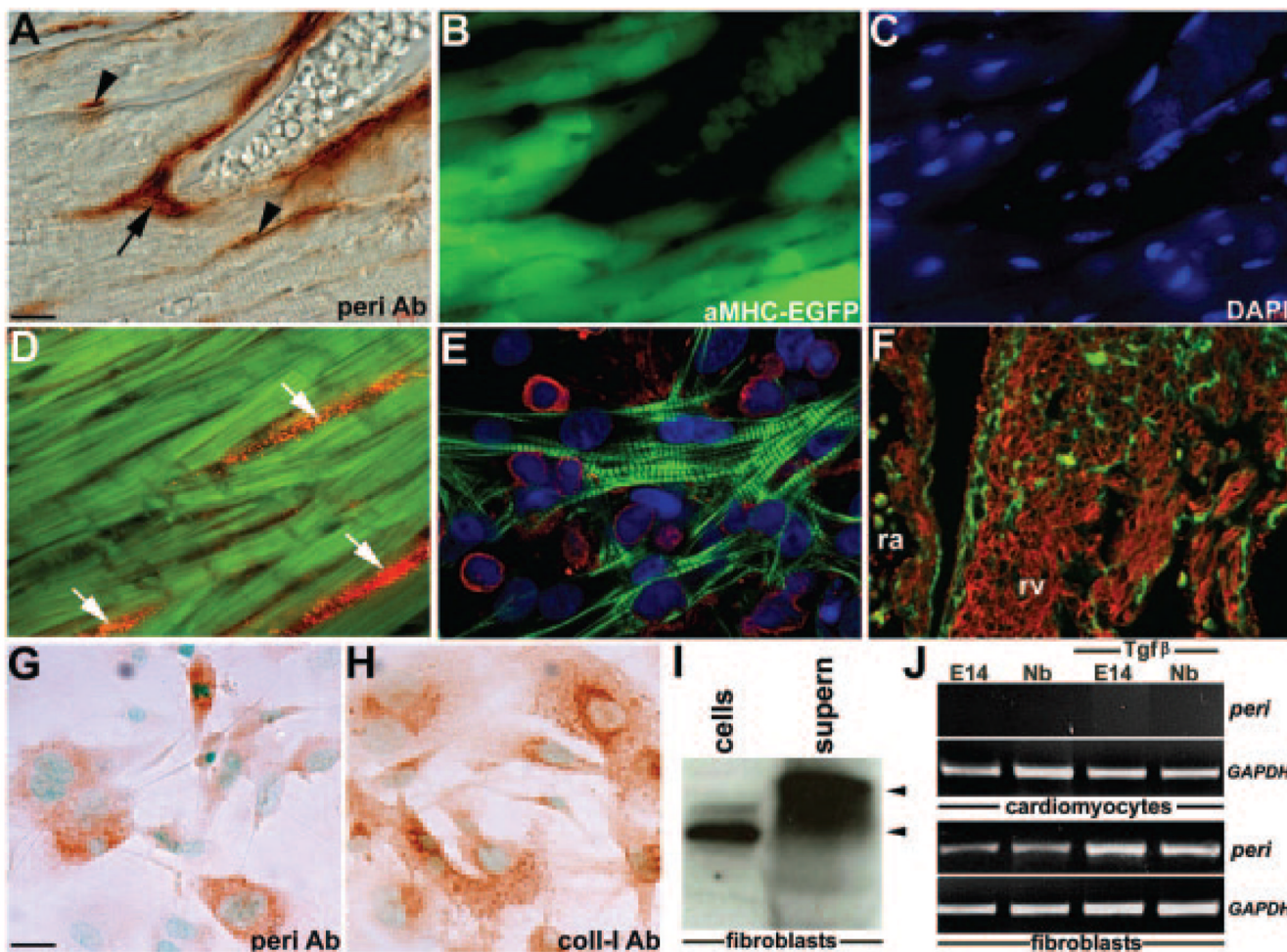


**Figure 2.** Periostin in cardiac fibroblast lineage. A through C, Periostin (A),  $\alpha$ MHC-EGFP (B), and 4', 6-diamidino-2-phenylindole (DAPI) (C) expression in the same section through adult  $\alpha$ MHC-EGFP heart. Periostin is restricted to vascular smooth muscle cells around coronaries (arrow in A) and cardiac fibroblasts (arrowheads in A) but absent from EGFP cardiomyocytes. D, Neonatal heart double-stained with anti-periostin (red) and cardiomyocyte-specific MF20 (green) antibodies (Ab). Fibroblasts (arrows) are periostin-positive, whereas cardiomyocytes are negative. E, Disassociated suspension of 4-day neonatal mouse hearts cocultured for 48 hours on collagen and stained for periostin (red) and sarcomeric actin (green). Note only fibroblasts are red (appear rounded as takes  $\approx$ 5 days to spread on collagen). F, E13.5 right atria and ventricle double-stained with anti-periostin and MF20 antibodies. Note there is no overlap (ie, yellow), and fibrillar-like periostin expression is present only in noncardiomyocyte lineages. G and H, Immunohistochemistry on cultured E14 cardiac fibroblasts reveals both periostin (G) and collagen type I (H) are present in cytoplasm. Negative controls lacking primary and/or secondary did not produce staining. (I) Western blotting showed that E14 cardiac fibroblasts express mainly  $\approx$ 82-kDa periostin isoform in cells and secrete larger  $\approx$ 90- and  $\approx$ 87-kDa isoforms. Equal loading of isolated cells and supernatant (supern) was verified via amido-black staining. J, Whereas E14 and newborn fibroblasts express periostin, cardiomyocytes lack expression following RT-PCR analysis. When treated with 1 ng/mL TGF $\beta$  overnight, periostin upregulation (7X) is observed in only fibroblasts. Note *GAPDH* is equally expressed in all samples (n=4 per genotype/age). Scale bars: 10  $\mu$ m (A and G).

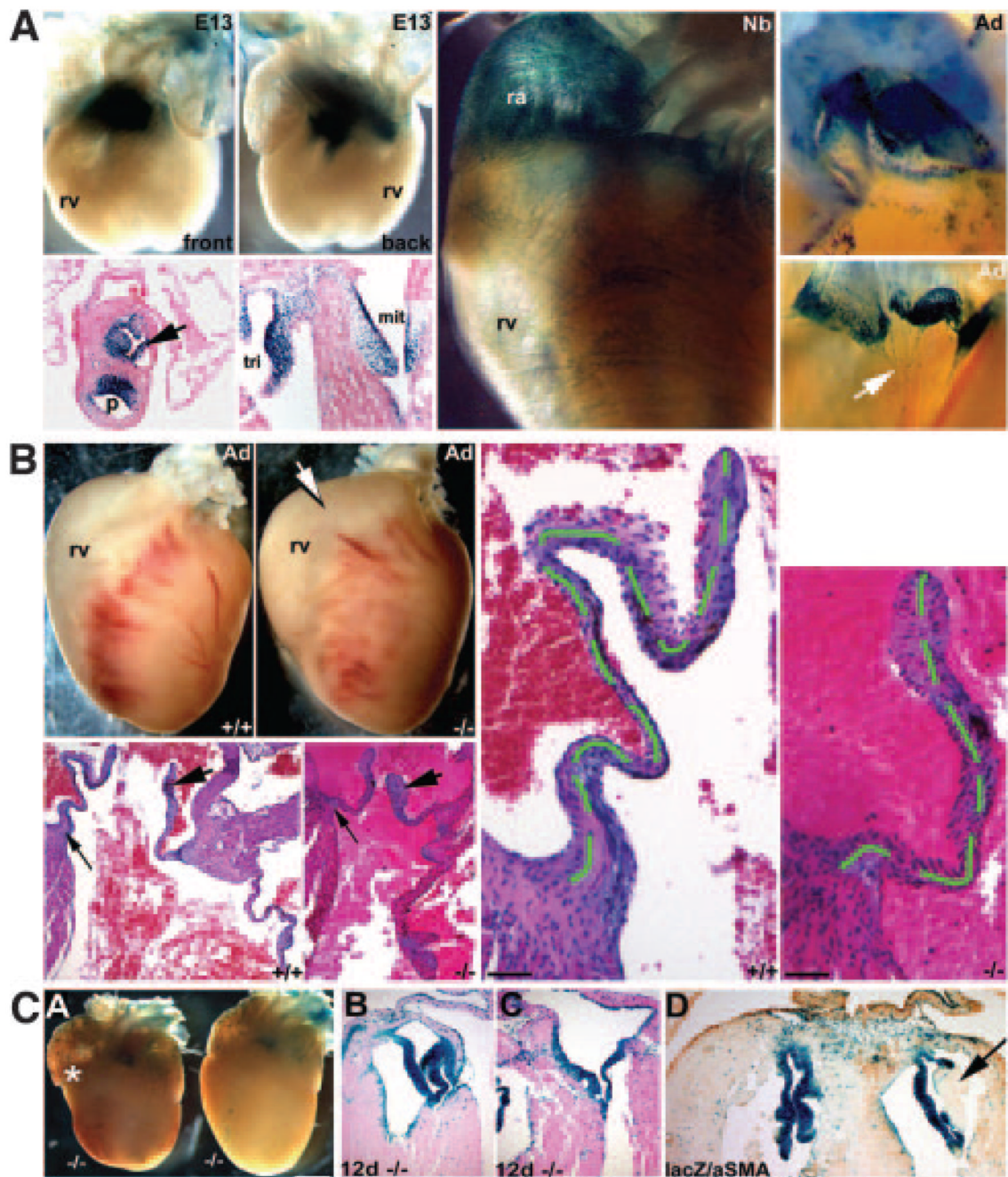


**Figure 3.**

Periostin knockout mouse hearts. a, Whole-mount *lacZ* staining of *peri<sup>lacZ</sup>+/-* E13, newborn, and 4-month-old (Ad) hearts. Note *peri<sup>lacZ</sup>* in E13 cushions (front and back). Histology reveals *peri<sup>lacZ</sup>* is confined to aortic, pulmonary (p), mitral, and tricuspid valves and cardiac fibroblasts but is absent from cardiomyocytes. b, Analysis of viable adult *peri<sup>lacZ</sup>*-null hearts (n=68; range 4 to 65 weeks). *peri<sup>lacZ</sup>*-null hearts (-/-) are dilated around the OFT (arrow). Histology revealed 100% of null leaflets were short and thickened. Scale in b, 100  $\mu$ m. c, In nonviable nulls ( $\approx$ 14%), neonatal mutant hearts are abnormally shaped (bulging right ventricle indicated by the asterisk), being rounded and lacking a distinct apex (A). Eosin counterstaining of transverse sections of 12-day neonatal *peri<sup>lacZ</sup>*-null hearts. Whereas viable *peri<sup>lacZ</sup>*-null mitral



valves are normal (B), nonviable *peri<sup>lacZ</sup>* heart (C) has its mitral septal leaflet tethered to the septum (n=8 abnormally shaped *peri<sup>lacZ</sup>* nulls examined).  $\alpha$ SMA coimmunostaining of *lacZ*-stained 2-week nonviable *peri<sup>lacZ</sup>*-null hearts revealed deposition of amorphous ECM in some leaflets (arrow in D) when compared with heterozygotes and viable *peri<sup>lacZ</sup>* nulls, and this amorphous ECM was acellular and negative for *lacZ* and  $\alpha$ SMA.

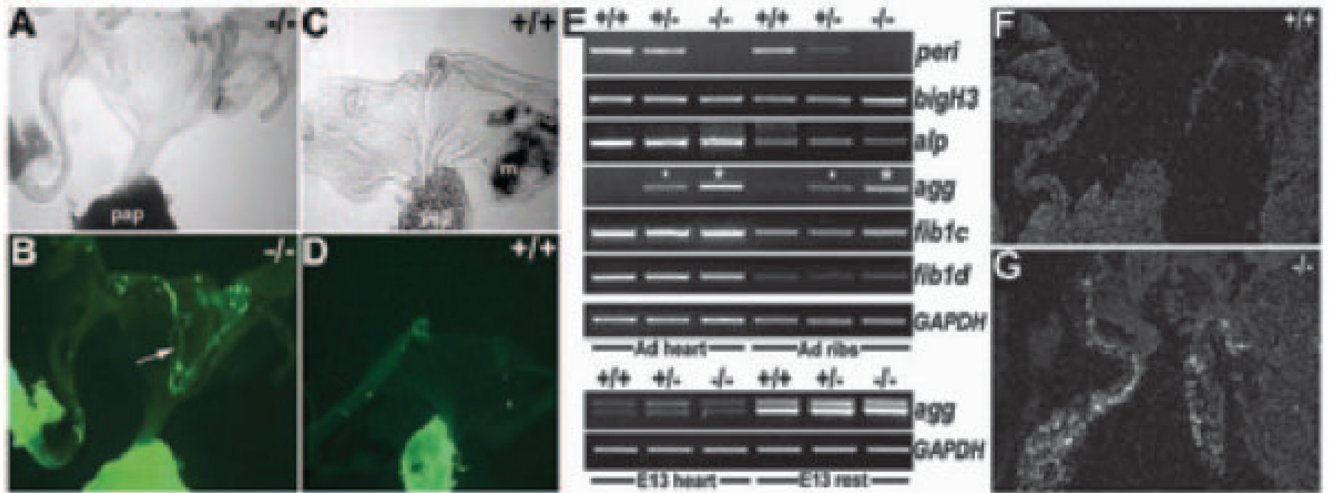


**Figure 4.** Characterization of surviving adult knockout heart phenotypes. Phase (A and C) and fluorescein isothiocyanate-MF20 (B and D) images of isolated and immunostained adult *peri<sup>lacZ</sup>*-null (A and B) and wild-type (C and D) leaflets. Note ectopic MF20-positive myocyte clusters in null valves (arrow in B) and papillary muscles (pap) appropriately express MF20. E, RT-PCR analysis of isolated E13 hearts and rests (whole embryo minus heart) and adult hearts and isolated rib cDNA samples (n=8 isolated E13 hearts/rest and 4 adult hearts/ribs from each respective genotype were pooled). Periostin mRNA is absent in *peri<sup>lacZ</sup>* nulls and  $\approx 50\%$  reduced in heterozygotes. Levels of *bigH3*, alkaline phosphatase (*alp*), fibulin-1c/1d are unaltered, but aggrecan is misexpressed in nulls (large\*). Aggrecan expression is also dose-dependently upregulated in adult heterozygotes (small\*). Significantly, aggrecan (mature and developmentally regulated isoforms) is expressed normally in E13 embryos. F and G, In situ revealed surviving adult *peri<sup>lacZ</sup>*-null valves (G) continue to express aggrecan, whereas normal littermates have switched it off (n=4).

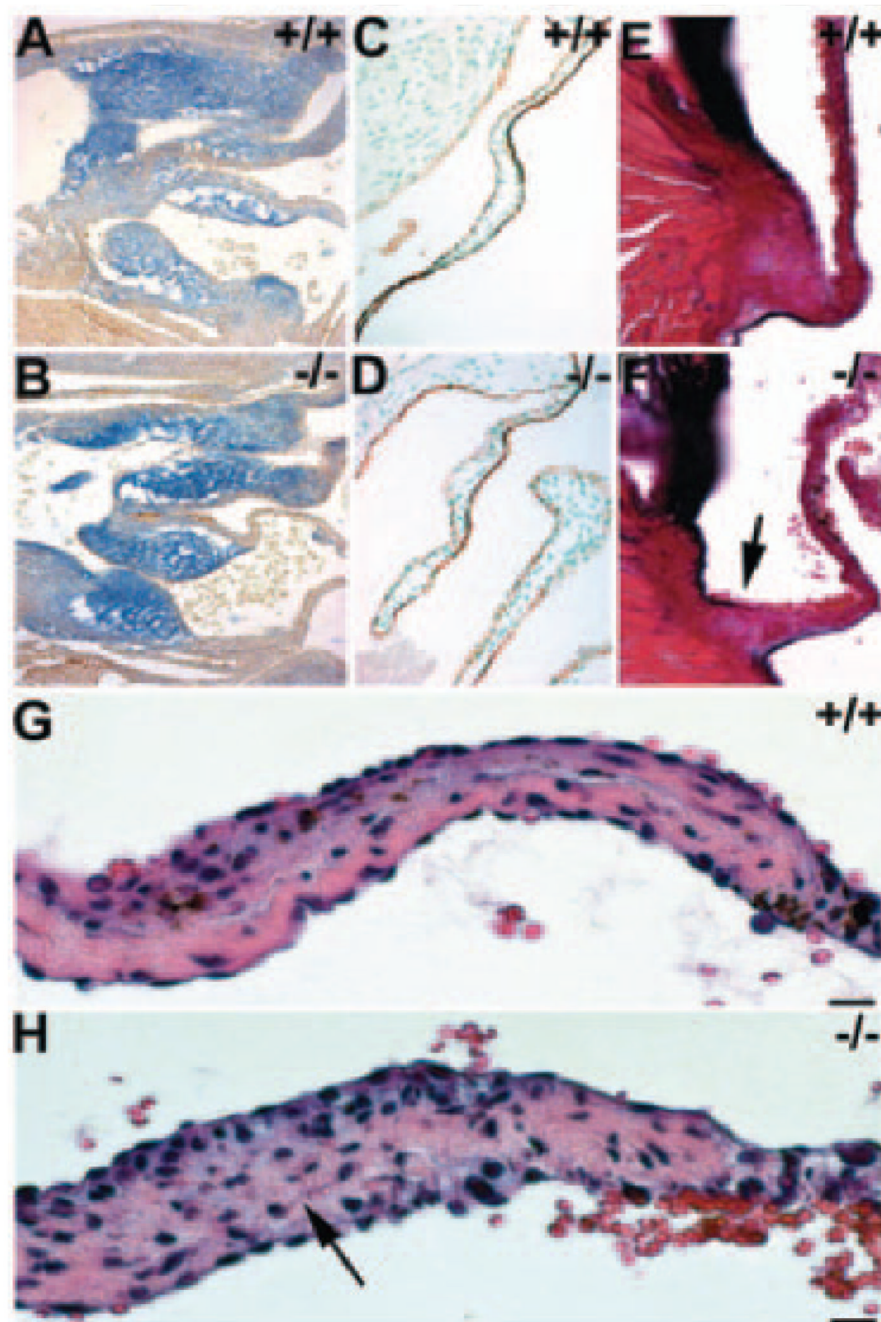


**Figure 5.** Null valvular pathology. Wild-type E12.5 (A) and *peri<sup>lacZ</sup>*-null (B) sagittal sections following alcian blue staining (pH 2.5) reveals increase in glycosaminoglycans in knockout OFT and AV cushions (n=5 per genotype). C and D, Platelet endothelial cell adhesion molecule immunostaining of wild-type and knockout leaflets indicates endothelium is intact. E and F, Resorcin-Fuchsin/van Gieson collagen/elastin staining shows null attachment sites are significantly undersized (arrow in F; n=7). G and H, Representative high-power views of hematoxylin/ eosin-stained viable +/+ adult (G) and *peri<sup>lacZ</sup>*<sup>-/-</sup> (H) mitral leaflets illustrating disorganization in nulls. Note that the defined, elongated pink collagen layer is absent in *peri<sup>lacZ</sup>* null (arrow in H). Scale: 10  $\mu$ m (G and H).

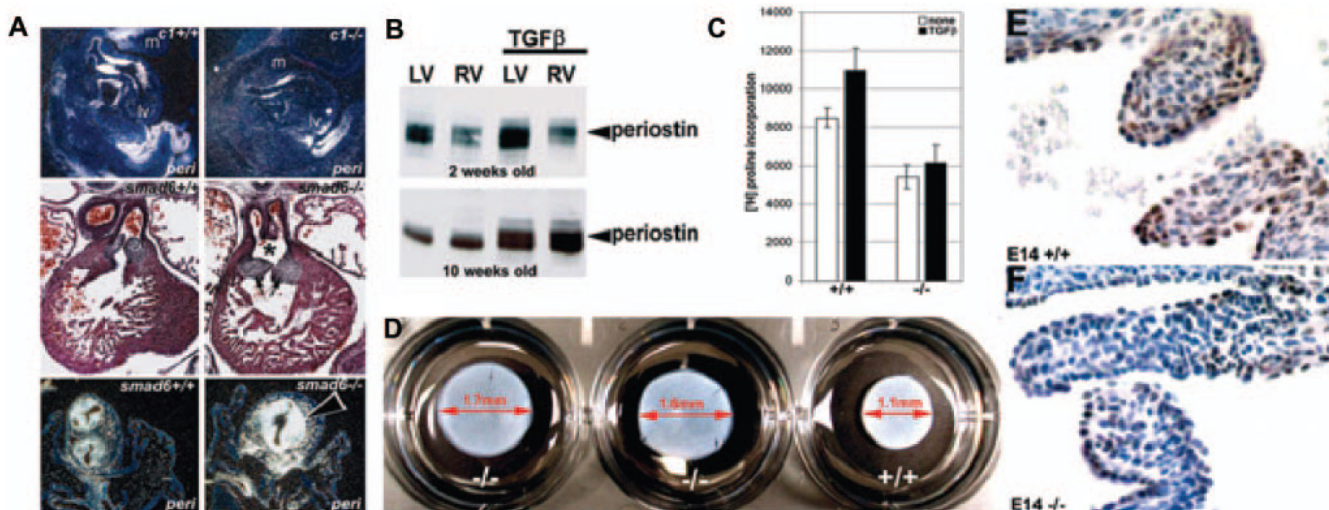


**Figure 6.**

Periostin is responsive to TGF $\beta$  but can also mediate TGF $\beta$  responsiveness. A, In situ demonstrated periostin is downregulated in E11.5 *Foxc1* (*c1*) knockouts and upregulated in E14 *Smad6* nulls. Note reduced periostin in *Foxc1*-null cushions, mandibular arch (m), and umbilical (top images) and upregulation in hyperplastic *Smad6*-null OFT cushions (bottom images). Hematoxylin/eosin staining of transverse sections (middle images) illustrate enlarged OFT cushions and the presence of persistent truncus arteriosus (\*) when inhibitory *Smad6* is removed. B, Western blot analysis revealed elevated periostin (9-fold) in 2- and 10-week  $\alpha$ MHC-TGF $\beta$ 1-expressing transgenic ventricles, compared with nontransgenic littermates. C,  $^3$ H-proline incorporation assays indicate collagen production is reduced in null E14 MEFs when compared with wild types (+/+ = 8663 $\pm$ 81 vs -/- = 5674 $\pm$ 94), and they fail to upregulate collagen synthesis with the addition of 1 ng/mL TGF $\beta$  (+/+ = 11 138 $\pm$ 77 vs -/- = 5286 $\pm$ 124). Data are expressed as counts per minute of [ $^3$ H]proline in  $10^4$  cells (n=3 independent lines/genotype). D, Three-dimensional collagen lattice contraction after 5 days in response to 0.1 ng/mL TGF $\beta$  was compared in 2 independent *peri*<sup>lacZ</sup> nulls vs +/+ littermate lines. Note the reduced contraction ( $\approx$ 18%) in both nulls, despite the presence of equal cell numbers ( $10^5$  cells/well). E and F, pSmad2,3 is attenuated in E14 *peri*<sup>lacZ</sup>-null leaflets (F) when compared with +/+ littermate controls (E) (n=4 per genotype).



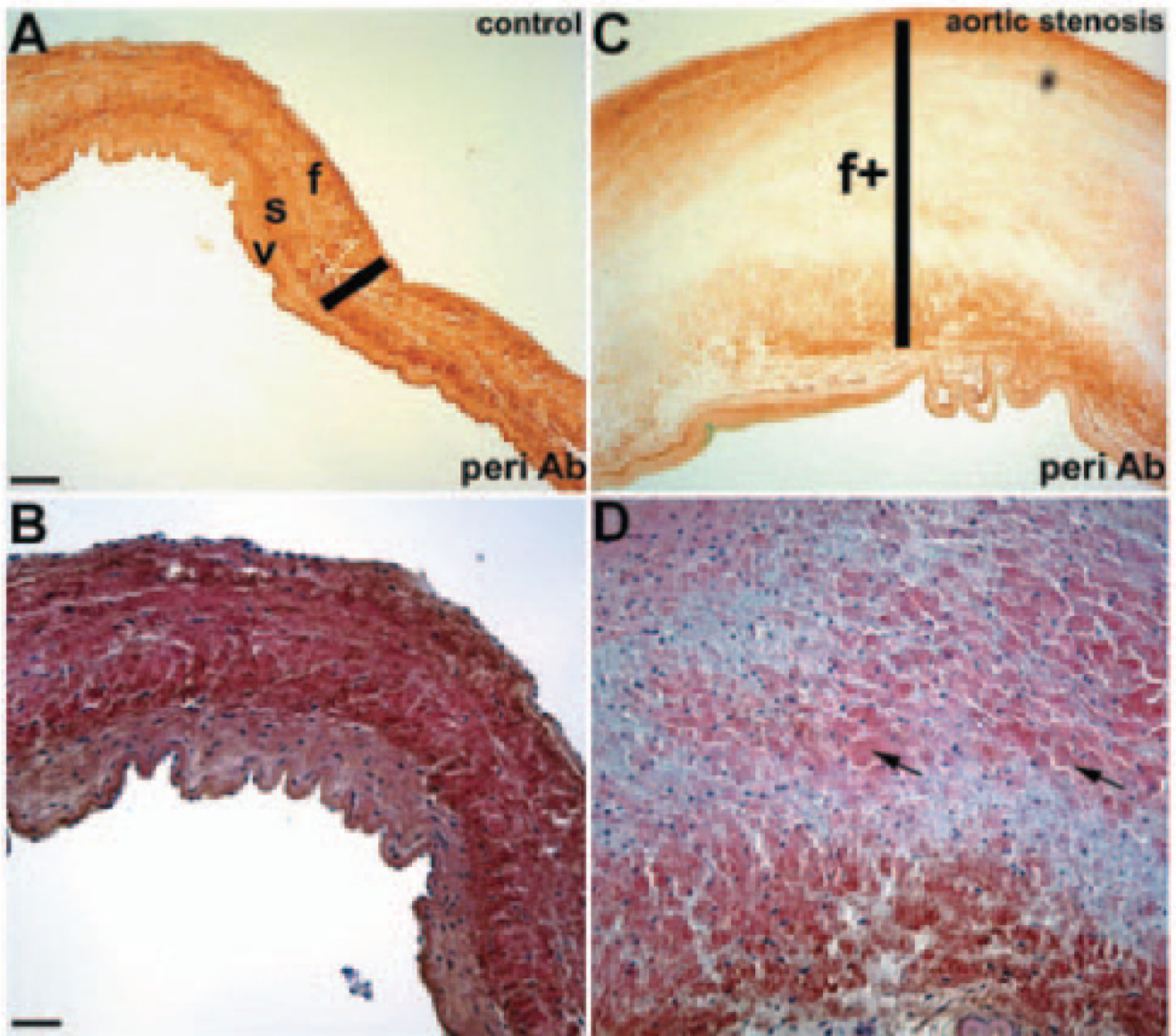


**Figure 7.**

Periostin expression and hematoxylin/eosin analysis in pediatric semilunar valves. A and B, Normal pediatric aortic valves demonstrate diffuse trilaminar periostin expression with increased expression in fibrosa (f) and spongiosa (s) relative to ventricularis (v). ECM fibrils (probably collagen) are elongated and arranged in a regular manner to provide a robust support structure. C and D, Stenosed aortic valves demonstrate overall markedly decreased periostin expression with an absence of expression in expanded fibrosa (bar in C) and disorganized ECM, as evidenced by increased valvular interstitial cells and disorganized collagen (arrows in D). Median age of samples is 6 years (range, 10 months to 15 years; n=9) compared with a median age of 9 years for controls (range, 3 to 14 years; n=6). A and C and B and D are viewed at similar magnifications. Scale bars: 1 mm (A); 50  $\mu$ m (B).



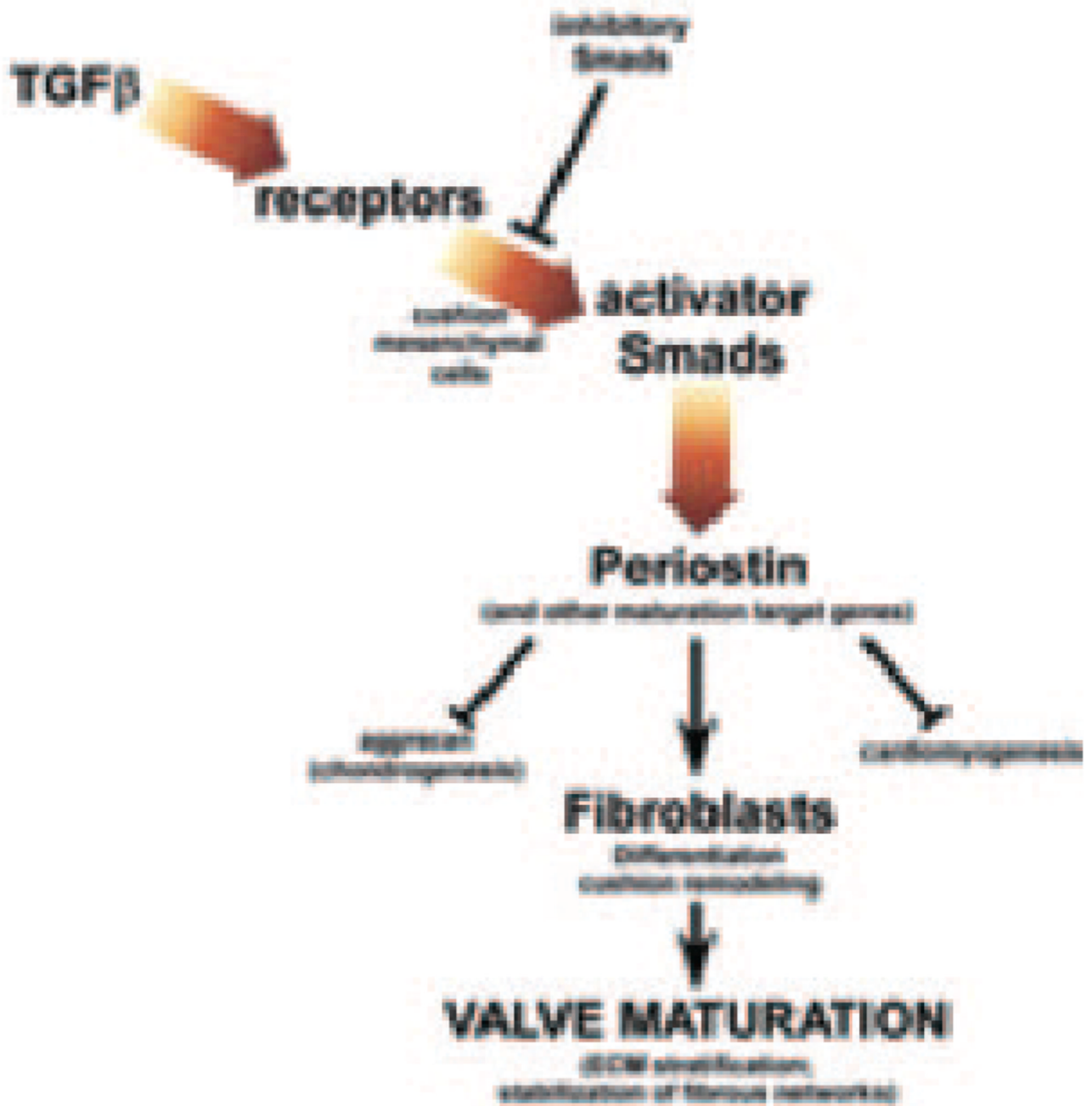


**Figure 8.**

Diagram of the proposed function of periostin. In response to TGFβ-mediated upstream signaling via phosphorylation of TGFβ-responsive receptors and Smad activation, periostin is upregulated (in addition to other established valvular remodeling factors, collagen, elastin, matrix metalloproteinases/ tissue inhibitors of metalloproteinase [MMPs/TIMPs], fibrillin-1). Both matrix-bound and secreted periostin acts to suppress nonvalvular phenotypes and promote valve mesenchymal differentiation and maturation by influencing ECM assembly, collagen realignment, and establishment of the valvular trilaminar structure in a TGFβ superfamily-dependent fashion.